Development 133, 4211-4218 (2006) doi:10.1242/dev.02602

Arabidopsis microRNA167 controls patterns of *ARF6* and *ARF8* expression, and regulates both female and male reproduction

Miin-Feng Wu, Qing Tian* and Jason W. Reed†

In flowering plants, diploid sporophytic tissues in ovules and anthers support meiosis and subsequent haploid gametophyte development. These analogous reproductive functions suggest that common mechanisms may regulate ovule and anther development. Two *Arabidopsis* Auxin Response Factors, ARF6 and ARF8, regulate gynoecium and stamen development in immature flowers. Wild-type pollen grew poorly in *arf6 arf8* gynoecia, correlating with *ARF6* and *ARF8* expression in style and transmitting tract. *ARF6* and *ARF8* transcripts are cleavage targets of the microRNA *miR167*, and overexpressing *miR167* mimicked *arf6 arf8* phenotypes. Mutations in the *miR167* target sites of *ARF6* or *ARF8* caused ectopic expression of these genes in domains of both ovules and anthers where *miR167* was normally present. As a result, ovule integuments had arrested growth, and anthers grew abnormally and failed to release pollen. Thus, *miR167* is essential for correct patterning of gene expression, and for fertility of both ovules and anthers. The essential patterning function of *miR167* contrasts with cases from animals in which miRNAs reinforce or maintain transcriptionally established gene expression patterns.

KEY WORDS: Auxin response factor, microRNA, Ovule, Anther, *Arabidopsis*

INTRODUCTION

Plant life cycles alternate between diploid sporophyte and haploid gametophyte phases. In flowering plants, the more prominent sporophyte supports meiosis and subsequent gametophyte development in specialized female and male organs within flowers. Ovules, the female sporophyte organs, support development of the embryo sac and growth of embryos and seeds after fertilization. Anthers, the male sporophyte organs, support the formation, development and subsequent release of pollen. Gametophyte development and successful reproduction thus require correct pattern formation of ovules and anthers.

Arabidopsis ovules initiate as finger-like structures on the flanks of carpel margin meristems at around floral stage 8 (Smyth et al., 1990). Megaspore mother cells, which later give rise to the female gametophyte, reside in the distal nucellus end of ovules. Proximal to the nucellus is the chalaza, where both inner and outer integuments initiate. Inner and outer integuments grow out to enclose the entire ovule as the ovule matures, and asymmetric growth of the outer integument causes the developing ovule to curve. After fertilization and embryo development, integuments form the seed coat. Ovules are connected to the placental tissues by funiculi, which supply nutrients to support ovule and seed growth (Schneitz et al., 1997; Skinner et al., 2004).

Stamen primordia initiate at floral stage 6 and form a filament that holds an anther at its distal end. Several distinct cell types in anthers are important for male gametogenesis and anther dehiscence (Goldberg et al., 1993; Smyth et al., 1990). Some of these undergo cell death or desiccation to allow dispersal of pollen grains at anthesis. Prior to anthesis, tapetum cells that coat the anther locule wall and septum cells between two anther locules are degraded. Stomium cells then break to allow pollen dispersal (Sanders et al., 1999).

Endogenous small non-coding RNAs called microRNAs (miRNAs) regulate several developmental events in *Arabidopsis* (Baker et al., 2005; Bao et al., 2004; Chen, 2004; Emery et al., 2003; Laufs et al., 2004; Mallory et al., 2004a; Williams et al., 2005). miRNA precursor genes (*MIR*s) are transcribed by RNA polymerase II in both animals and plants (Kurihara and Watanabe, 2004; Lee et al., 2004; Xie et al., 2005). DICER-LIKE 1 (DCL1), an *Arabidopsis* DICER RNase III family homolog, cleaves the pri-miRNA and pre-miRNA hairpin precursors to produce a miRNA:miRNA* duplex in the nucleus (Jones-Rhoades et al., 2006). The duplex is transported to the cytoplasm where the mature miRNA is incorporated into the RNA-induced silencing complex (RISC). The RISC complex then identifies target mRNAs with specificity provided by base pairing between the miRNA and the target site (Bartel, 2004).

Most plant miRNAs have high sequence complementarity to their target binding sites, allowing a straightforward prediction of the genes they regulate (Rhoades et al., 2002). In most cases, plant miRNAs shut down their target gene activities by transcript cleavage (Axtell and Bartel, 2005; Schwab et al., 2005). Overexpressing *MIR* precursor transcripts in transgenic plants decreased the corresponding target gene transcript levels (Schwab et al., 2005). In addition, cleavage products of computationally predicted miRNA targets have been detected in wild-type plants (Allen et al., 2005; Kasschau et al., 2003; Mallory et al., 2005; Xie et al., 2005). Nevertheless, miRNAs can act by other regulatory mechanisms, including translational inhibition and methylation-induced gene silencing (Bao et al., 2004; Bartel, 2004; Chen, 2004; Kurihara and Watanabe, 2004).

More than half of the known *Arabidopsis* miRNA target genes encode transcription factors, suggesting that miRNAs regulate various developmental processes (Jones-Rhoades et al., 2006). The importance of plant miRNAs is further supported by the finding that most *Arabidopsis* miRNA families are conserved among other

University of North Carolina at Chapel Hill, Department of Biology, CB #3280, Coker Hall, Chapel Hill, NC 27599-3280, USA.

*Present address: Monsanto, St Louis, MO 63146, USA
†Author for correspondence (e-mail: jreed@email.unc.edu)

Accepted 30 August 2006

species of land plants, both vascular and, in some cases, lower plants (Axtell and Bartel, 2005; Floyd and Bowman, 2004; Reinhart et al., 2002; Rhoades et al., 2002; Sunkar et al., 2005).

Among miRNA targets are several *ARF* genes encoding Auxin Response Factors. *ARF6* and *ARF8* are targeted by *miR167*, whereas *ARF10*, *ARF16* and *ARF17* are targeted by *miR160* (Mallory et al., 2005; Rhoades et al., 2002; Wang et al., 2005). ARF proteins bind to auxin response promoter elements and mediate gene expression responses to the plant hormone auxin (Hagen and Guilfoyle, 2002; Liscum and Reed, 2002; Mallory et al., 2005; Tiwari et al., 2003). Different ARF proteins regulate embryogenesis, root development and floral organ formation (Hardtke and Berleth, 1998; Hardtke et al., 2004; Mallory et al., 2005; Sessions et al., 1997; Wang et al., 2005).

We previously found that *ARF6* and *ARF8* regulate flower maturation (Nagpal et al., 2005). Flowers of *arf6 arf8* double loss-of-function mutant plants were arrested at stage 12, just before wild-type flower buds normally open. Stamens of *arf6 arf8* flowers were short, and anthers did not dehisce to release pollen. The double mutant anther indehiscence was due to a lack of jasmonic acid (JA) production, and pollen release could be restored by spraying the flower buds with JA or its precursors. *arf6 arf8* double mutant flowers were also female sterile and their stigmatic papillae did not elongate as did those of wild-type flowers. Single loss-of-function *arf6* or *arf8* mutants had only subtly reduced fecundity, resulting from shorter stamen filaments and delayed anther dehiscence, indicating that ARF6 and ARF8 act largely redundantly.

To determine the developmental functions of *miR167*, we have overexpressed *MIR167*-coding sequences, mutated *ARF6* and *ARF8* to make them immune to *miR167*-mediated effects, and studied the expression of *MIR167*, *ARF6* and *ARF8* genes. Our results indicate that *miR167* regulates the pattern of *ARF6* and *ARF8* expression, which is vital for both ovule and anther development.

MATERIALS AND METHODS

Plant materials and constructs

Most plants used in this work were of the Columbia (Col-0) ecotype. *arf6-2*, *arf8-3* and *arf6-2 arf8-3* mutants were isolated and described previously (Nagpal et al., 2005). The *ino-1* mutant (Villanueva et al., 1999) was of the Landsberg *erecta* ecotype.

MIR167a (At3g22886; stem-loop sequence accession number, MI0000208), *MIR167b* (At3g63375; stem-loop accession number, MI0000209), *MIR167c* (stem-loop accession number, MI0001088) and *MIR167d* (stem-loop accession number, MI0000975) were PCR amplified from wild-type genomic DNA using the following primers:

MIR167a, 5′-CACCCACTTTCGACCCTTAAACTCTCCA-3′ and 5′-TGAAGCTAGGAAAGAGGAGCTTTG-3′;

MIR167b, 5′-CACCTCAGGCTTCTTTAATTCGTGGTG-3′ and 5′-AACTTAGACTGTGCAAAGCCAAA-3′;

MIR167c, 5′-CACCCCATGGGTGAGAAAGTGAAAA-3′ and 5′-TCATGATTGTCACACTAGCACAA-3′; and

MIR167d, 5′-CACCTGAATGAAACTGTCCAAACACA-3′ and 5′-CGTCGCTAGCTACCAACAAA-3′.

PCR products were cloned into pENTR/D-TOPO (Invitrogen) and then subcloned into binary vector pB7WG2 (Karimi et al., 2002) by LR clonase (Invitrogen).

A genomic *ARF6* (*gARF6*) fragment including the 5′ and 3′ regulatory sequences (chromosome 1 positions 10693520-10680841) was cut out from BAC clone T4K22 with *Bam*HI and subcloned into pBS SK$^-$ (Stratagene) (Nagpal et al., 2005). The *miR167* target site on *ARF6* was mutated by PCR using primers: 5′-GACCCTGTGCGTAGTGGATGG-CAGCTGGTATTTG-3′ and 5′-CAAATACCAGCTGCCATCCACTACG-CACAGGGTC-3′. Both *gARF6* and the mutated *ARF6* (*mARF6*) were cloned into binary vector pBAR (Holt et al., 2002). Genomic *ARF8* (*gARF8*) was obtained from BAC clone K15O15 by PCR (chromosome 5 position 14645242-14652007) in three fragments using the following primer pairs, and then ligated together: 5′-CTCGAGTGAGAACTGAGGCTGGCTTT-3′ and 5′-GTCTAATTCAACTTCAAGAA-3′; 5′-TCTTCCTTCTCTCC-ACTGTATCG-3′ and 5′-GACCCTCTTCAGAGCTCTACTCA-3′; and 5′-CACCATCGATCATGCTGGCACATCATCTTT-3′ and 5′-CTCGA-GCTAGGCACTGTTTATG-3′. *mARF8* was obtained by mutating the *miR167* target site by the same method as for *mARF6*. Both *gARF8* and *mARF8* were first cloned into pENTR/D-TOPO (Invitrogen) and then into binary vector pKWG (Karimi et al., 2002) by LR clonase (Invitrogen).

gARF6, *mARF6*, *gARF8* and *mARF8* fragments, excluding their stop codons and 3′ untranslated regions, were cloned into pENTR/D-TOPO (Invitrogen) and then introduced into pGWB3 (a kind gift from Dr Tsuyoshi Nakagawa, Shimane University, Japan) by LR clonase (Invitrogen) to obtain the protein GUS fusions.

$P_{MIR167a}$, $P_{MIR167b}$, $P_{MIR167c}$ and $P_{MIR167d}$ were PCR amplified from wild-type genomic DNA using the following primers:

$P_{MIR167a}$, 5′-CACCAAGTTTCGAGTAGACCGTGA-3′ and 5′-TCA-GATGCCGGTGCACCATA-3′;

$P_{MIR167b}$, 5′-CACCAGGGTAGAGGGTTTCTCAAG-3′ and 5′-TTG-TGGACTTGTCTTCAAAA-3′;

$P_{MIR167c}$, 5′-CACCCGTTGTGTGGTGTTTCCAAC-3′ and 5′-TAC-ATGGTATACATACAGACATGA-3′; and

$P_{MIR167d}$, 5′-CACCTCACGTTTCTATGGACCCAAT-3′ and 5′-TAG-ATAATTGAAAAAGAATGAGAAG-3′.

These promoters were cloned into pENTR/D-TOPO (Invitrogen) and subcloned into binary vector pBGWFS7 (Karimi et al., 2002) to produce P_{MIR167}*:GFP-GUS* constructs. Only GUS activity was assayed in plants carrying these constructs.

Northern blots and in situ hybridization

Total cellular RNA was isolated from flower clusters of long-day-grown plants by Trizol reagent (Invitrogen). RNA gel blot analysis was performed as previously described (Tian et al., 2003). *ARF6* (coding region position 1346-2211) and *ARF8* (coding region position 1151-2106) probes were amplified from cDNA with the following primers: *ARF6*, 5′-CGGA-ATTCAGGCATTGATCCTGCAAAAG-3′ and 5′-CGGGATCCAAGG-TTTGACATTCCGTTCG-3′; and *ARF8*, 5′-CGGGATCCGAAGGGGT-GATTTGGGAAGT-3′ and 5′-CTCGAGGTTGGACGAGTTAATCTG-TCC-3′. A probe recognizing *Arabidopsis* β-tubulin 4 (At5g44340) was used as a loading control in RNA gel blot hybridizations.

For low molecular weight RNA, 30 μg of total cellular RNA was suspended in 20 μl loading buffer (95% formamide, 5 mM EDTA, 0.025% SDS, 0.025% bromophenol blue and 0.025% xylene cyanol FF) and separated in 15% denaturing polyacrylamide gel containing 8 M urea. Antisense *miR167* (5′-TAGATCATGCTGGCAGCTTCA-3′) and U6 snRNA probes (5′-CTCGATTTATGCGTGTCATCCTTGC-3′) were end labeled by T4 polynucleotide kinase (New England Biolabs) in the presence of γ^{32}P-ATP.

In situ hybridization was performed as previously described (Long and Barton, 1998). *ARF6* and *ARF8* fragments used in northern blots were cloned into plasmid pGEM-T (Promega). Probes were labeled by in vitro transcription with SP6 polymerase using a DIG RNA labeling kit (Roche). Wild-type and *mARF6* hybridizations were done together, so as to increase comparability of results. *INNER NO OUTER* probe was amplified from wild-type flower cDNA using primers described by Sieber et al. (Sieber et al., 2004) and cloned into pGEM-T (Promega).

Histology and microscopy

Flower X-gluc staining was performed as described by Sessions et al. (Sessions et al., 1999), and the concentration of potassium ferrocyanide and ferricyanide used depended on the constructs. For *MIR167* promoter:GFP-GUS lines, the concentration used was 5 mM each. For *ARF6* and *ARF8* protein:GUS fusions, it was 0.5 mM each for ovules and 0.2 mM each for flowers.

For tracking pollen tube growth, stigmas were dusted with pollen from *LAT52:GUS* plants (Johnson et al., 2004). Twenty-four hours after pollination, carpel walls were removed and gynoecia were stained with X-gluc overnight at 37°C.

Ovules for DIC microscopy were fixed in 3:1 ethanol:acetic acid for 15 minutes, incubated in 70% ethanol for another 15 minutes, cleared in chlorohydate solution (chlorohydrate:water, 8:2), and observed under DIC microscopy. Scanning electron microscopy was performed as previously described (Nagpal et al., 2005). Anthers were fixed and sectioned based on methods described by Ellis et al. (Ellis et al., 2005).

RESULTS

ARF6 and *ARF8* are required to support pollen tube growth

Our previous analyses of promoter:GUS plants suggested that both *ARF6* and *ARF8* were expressed in multiple flower organs, but would not have revealed effects of *miR167* or other regulatory elements missing from the promoter:GUS constructs. We therefore analyzed the expression patterns of *ARF6* and *ARF8* in wild-type flowers by in situ hybridization (Fig. 1). We also analyzed X-gluc staining patterns in plants carrying genomic translational fusions to the *GUS* reporter gene (Fig. 2). These *gARF6:GUS* and *gARF8:GUS* constructs were able to increase fecundity of an *arf8* null mutant (data not shown), suggesting that they were partially functional (although, as discussed below, *miR167*-resistant versions conferred weaker phenotypes than did unfused genes). In most tissues, staining patterns of the GUS fusions were very similar to the distribution of transcripts shown by in situ hybridization.

In wild-type flowers, *ARF6* transcript was present in the carpel medial ridge (which later forms the transmitting tract for pollen tube growth), in placental tissues, and in young ovule primordia as they emerged (Fig. 1B,D). As integuments initiated on the flanks of ovules (ovule stage 2-II), *ARF6* transcript became restricted to the ovule funiculus and the placental tissues, and was excluded from the integuments and the nucellus (Fig. 1E,F). These expression patterns persisted at least through flower stage 12, just before fertilization would normally occur. *ARF6* transcript was also detected at a low level in the vasculature of flower stems and stamen filaments, in petals, and in nectaries (Fig. 1A,C). Consistent with the in situ hybridization data, *gARF6:GUS* expression was detected in the transmitting tract, the ovule funiculi and nectaries, and faintly in the stamen filaments (Fig. 2A-E).

ARF8 was expressed in a similar pattern to *ARF6*, with strong expression in the funiculus and placenta (Fig. 1J). *ARF8* was also detected in stigmatic papillae in flowers approaching anthesis (data not shown). Similarly, g*ARF8:GUS* was expressed in the transmitting tract, placenta, funiculi and stamen filaments (Fig. 2K,M). Stigmatic papillae expression was also detected in some strongly expressing *gARF8:GUS* lines (data not shown). In addition, we detected weak X-gluc staining in the style and in the valves of both *gARF6:GUS* and *gARF8:GUS* plants, but we did not detect *ARF6* or *ARF8* transcripts in these tissues by in situ hybridization.

Expression of *ARF6* and *ARF8* in style, transmitting tract and funiculus suggests that ARF6 and ARF8 may regulate fertilization rather than gametophyte development. To explore why *arf6 arf8* flowers were female sterile, we pollinated wild-type and *arf6 arf8* stigmas with pollen from the *LAT52:GUS* reporter line (Johnson et al., 2004). Whereas pollen grew efficiently in wild-type transmitting tracts and fertilized the majority of ovules, pollen tubes elongated very little in *arf6 arf8* transmitting tracts (Fig. 4M). These results indicate that ARF6 and ARF8 may act within the stigma, style or transmitting tract to regulate the production of some component necessary for pollen tube germination or growth.

MIR167 genes can decrease *ARF6* and *ARF8* transcript levels

ARF6 and *ARF8* mRNA cleavage products ending within the *miR167* target site have been detected in wild-type plants (Allen et al., 2005; Jones-Rhoades and Bartel, 2004; Rhoades et al., 2002). To test whether *miR167* targets only these two genes, we made transgenic plants expressing the stem-loop regions of each of the

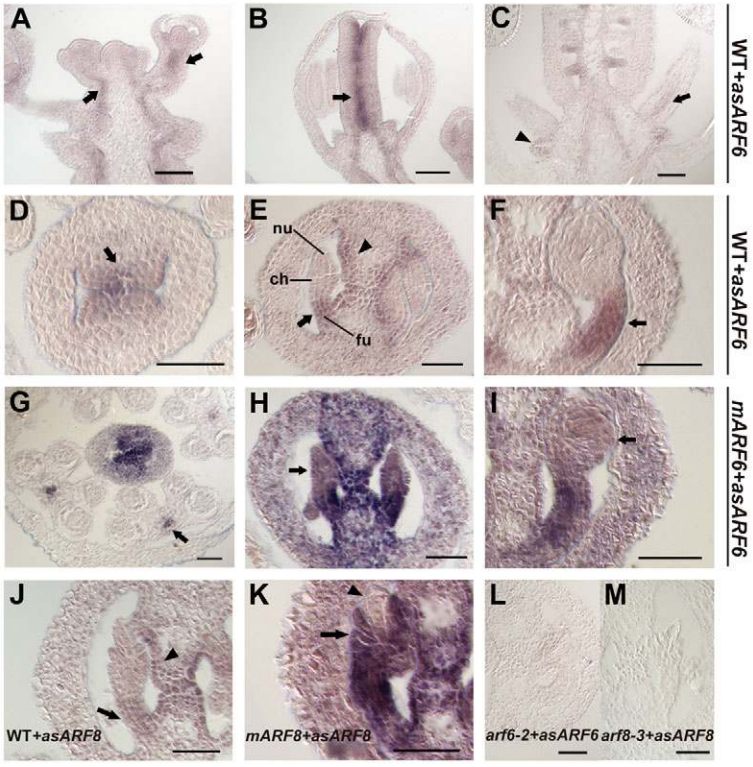

Fig. 1. *ARF6* and *ARF8* mRNA expression patterns. (**A-I**,**L**) Sections of wild-type (A-F), *mARF6* (G-I) and *arf6-2* (L) flowers hybridized with an antisense *ARF6* probe. (**J**,**K**,**M**) Sections of wild-type (J), *mARF8* (K) and *arf8-3* (M) flowers hybridized with an antisense *ARF8* probe. (A) Longitudinal section of inflorescence. Arrows indicate vasculature. (B) Longitudinal section of stage 9 flower. Arrow indicates *ARF6* expression in the medial ridge of carpels. (C) Longitudinal section of a stage 12 flower. Arrow indicates stamen filament vasculature; arrowhead indicates nectary. (D) Cross section of a stage 9 flower gynoecium. Arrow indicates the medial ridge of carpels. (E) Stage 2-II ovule. Arrow indicates funiculus; arrowhead indicates the placental region. (F) Stage 3-I ovule. Arrow indicates funiculus. (G) Cross section of a stage 9 flower bud. Arrow indicates anther vasculature. (H,I) Stage 2-III (H) and stage 3 (I) ovules. Arrows indicate the integument and nucellus regions. (J) Stage 2-II ovule. Arrow indicates funiculus; arrowhead indicates the placental region. (K) Stage 3-I ovule. Arrow indicates integuments; arrowhead indicates nucellus. ch, chalaza; fu, funiculus; nu, nucellus. Scale bars: 60 μm in A-C,G; 30 μm in D-F,H-M.

DEVELOPMENT

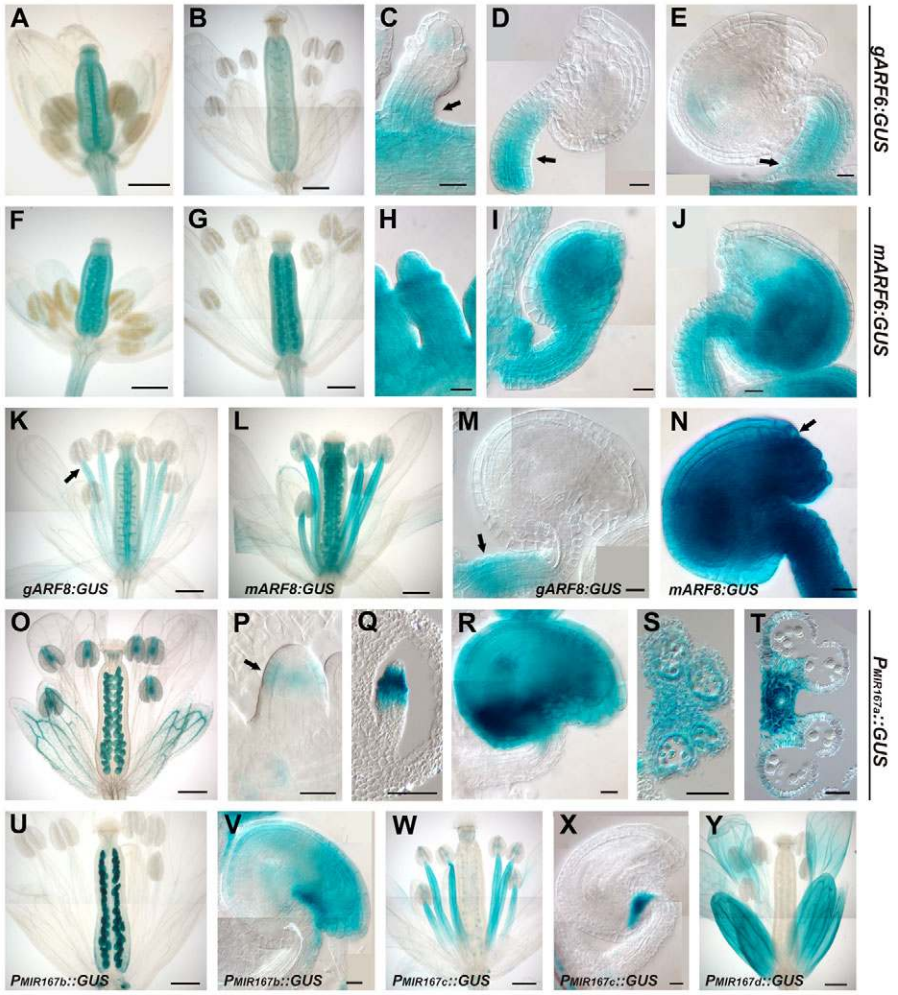

Fig. 2. Expression patterns of *gARF6*, *mARF6*, *gARF8* and *mARF8* protein:GUS fusions, and *MIR167* promoter::GUS fusions. (**A-E**) *gARF6:GUS*. (**F-J**) *mARF6:GUS*. (**K**,**M**) *gARF8:GUS*. (**L**,**N**) *mARF8:GUS*. (**O-T**) $P_{MIR167a}$*::GUS*. (**U**,**V**) $P_{MIR167b}$*::GUS*. (**W**,**X**) $P_{MIR167c}$*::GUS*. (**Y**) $P_{MIR167d}$*::GUS*. (A,B) *gARF6:GUS* staining patterns in stage 11 (A) and stage 13 (B) flowers. (C-E) *gARF6:GUS* expression in stage 2-III (C), stage 3-I (D) and stage 4-I (E) ovules. Arrows indicate funiculus. (F,G) *mARF6:GUS* expression in stage 11 (F) and stage 13 (G) flowers. (H-J) *mARF6:GUS* expression in ovules. Ovule development stages in H,I,J are equivalent to those in C,D,E, respectively. (K) *gARF8:GUS* staining in a stage 13 flower. Arrow indicates stamen filament expression. (L) *mARF8:GUS* staining in a stage 13 flower. (M) *gARF8:GUS* staining in a stage 4-I ovule funiculus (arrow). (N) *mARF8:GUS* expression in a stage 4-I ovule. Arrow indicates reduced outer integument growth. (O) $P_{MIR167a}$*::GUS* expression in a stage 13 flower. (P-R) $P_{MIR167a}$*::GUS* in stage 1-II (P), stage 2-III (Q) and stage 3-IV (R) ovules. (S,T) $P_{MIR167a}$*::GUS* expression in floral stage 10 (S) and stage 13 (T) anthers. (U,V) $P_{MIR167b}$*::GUS* expression in a stage 13 flower (U) and a stage 4-I ovule (V). (W,X) $P_{MIR167c}$*::GUS* expression in a stage 13 flower (W) and a stage 4-I ovule (X). (Y) $P_{MIR167d}$*::GUS* expression in a stage 13 flower. Scale bars: 0.3 mm in A,B,F,G,K,L,O,U,W,Y; 12 μm in C-E, H-J,M,N,P,R,V,X; 30 μm in Q,S,T.

four predicted *Arabidopsis MIR167* precursor genes behind the strong *Cauliflower Mosaic Virus 35S* promoter (P_{35S}*::MIR167a*, *b*, *c* and *d*). Only P_{35S}*::MIR167a* caused twisted leaves, short inflorescences and arrested flower development, thereby fully recapitulating *arf6 arf8* mature plant phenotypes (Fig. 3B,C and Table 1). We did not examine seedling or root phenotypes in these sterile plants. P_{35S}*::MIR167b* and P_{35S}*::MIR167c* caused weaker mutant phenotypes, whereas P_{35S}*::MIR167d* plants all appeared identical to wild-type plants (Fig. 3B,C and Table 1). The phenotypic strengths of plants expressing different *MIR167* precursor genes correlated with the amount of mature *miR167* produced, and with the degree of reduction of *ARF6* and *ARF8* transcript levels (Fig. 3D). These results confirm that *miR167* can remove or destabilize *ARF6* and *ARF8* transcripts in vivo. No additional leaf or flower phenotype was observed in transgenic plants carrying any of the four constructs, suggesting that *miR167* targets only *ARF6* and *ARF8* in adult leaves, inflorescences and flowers.

miR167-immune *mARF6* and *mARF8* flowers are sterile

To elucidate the developmental function of *miR167*, we introduced eight translationally silent mutations into *miR167* target sites in both *ARF6* and *ARF8* coding sequences, in the context of their normal 5′ and 3′ flanking sequences (Fig. 3A, *mARF6* and *mARF8*), and transformed these constructs into wild-type plants. These mutations disrupted base pairing between *miR167* and its target site, and should therefore render *mARF6* and *mARF8* transcripts immune to *miR167*-mediated turnover. Corresponding wild-type genomic constructs (*gARF6* and *gARF8*) increased fecundity of the loss-of-function mutants (Nagpal et al., 2005) (data not shown), indicating that these genomic constructs were functional. *mARF6* and *mARF8* T1 plants had the same spectrum of phenotypes (Fig. 4, see also Fig. S1 in the supplementary material), supporting our previous conclusion that *ARF6* and *ARF8* have similar activities (Nagpal et al., 2005). We focus here on our phenotypic studies of *mARF6* plants.

Table 1. Summary of P_{35S}*::MIR167* T1 plant phenotypes

Gene	Predicted sequence*	Strong (*arf6 arf8*-like)	Medium	Weak	No phenotype
MIR167a	5′-UGAAGCUGCCAGCAUGAUCUA-3′	100	12	0	0
MIR167b	5′-UGAAGCUGCCAGCAUGAUCUA-3′	0	3	101	8
MIR167c	5′-UUAAGCUGCCAGCAUGAUCUU-3′	0	0	91	7
MIR167d	5′-UGAAGCUGCCAGCAUGAUCUGG-3′	0	0	0	109

*(Jones-Rhoades and Bartel, 2004; Rhoades et al., 2002).

DEVELOPMENT

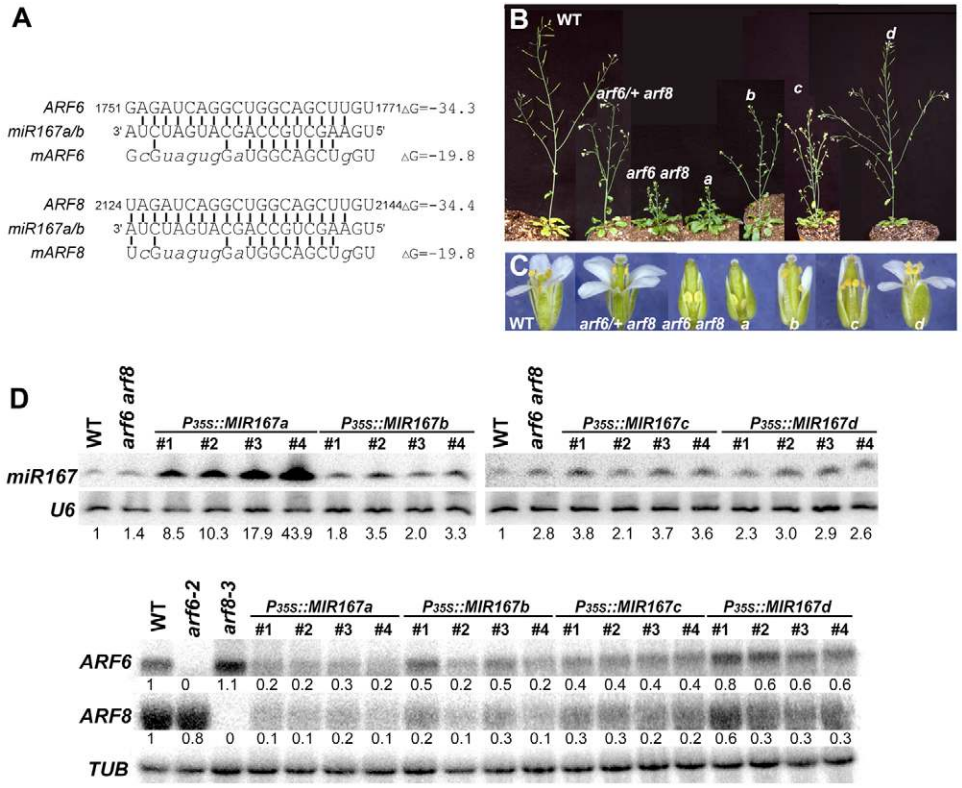

Fig. 3. Effects of overexpressing *MIR167* genes. (**A**) Sequences of *miR167* target sites on *ARF6* and *ARF8* mRNA, and the mutated target sites of *mARF6* and *mARF8*. The Watson-Crick base pairings to the *miR167* sequence are shown. ΔG (kcal/mol) was calculated by Mfold (Zuker, 2003). Mutated nucleotides are in lower case. (**B**) Phenotypes of plants overexpressing four different *MIR167* genes. From left to right: wild type (WT), *arf6/+ arf8*, *arf6 arf8*, P_{35S}*::MIR167a* (*a*), P_{35S}*::MIR167b* (*b*), P_{35S}*::MIR167c* (*c*) and P_{35S}*::MIR167d* (*d*). (**C**) Stage 13 flowers of P_{35S}*::MIR167* plants. Genotypes are the same as in B. (**D**) Northern blot analyses of *MIR167*-overexpressing transgenic plant flowers. U6 snRNA and β-tubulin are included as loading controls. Numbers beneath lanes indicate relative transcript levels normalized to loading controls.

The severity of phenotypes of *mARF6* plants correlated with the level of *mARF6* transcript being expressed (Fig. 4A). *mARF6-I* transgenic plants with the highest *ARF6* levels (12 out of 63 T1 plants) had small leaves and sterile flowers (Fig. 4A,B; see also Fig. S2 in the supplementary material). *mARF6-II* plants, with *ARF6* levels higher than wild-type plants but lower than *mARF-I* plants (36/63), had slightly smaller leaves than wild-type plants and sterile flowers (Fig. 4A,B; Fig. S2 in the supplementary material). *mARF6-III* plants (15/63), with similar *ARF6* levels to wild-type plants, had leaves similar in size to those of *mARF6-II* or wild-type plants, but did produce seeds (Fig. 4A,B; Fig. S2 in the supplementary material). However, *mARF6-III* seeds were small and could not germinate. As described below, embryos in these seeds were arrested.

Wild-type plants transformed with genomic *ARF6* or *ARF8* constructs, or expressing the wild-type *ARF6*-coding sequence behind the CaMV 35S promoter (P_{35S}*::ARF6*) had fertile flowers despite having *ARF6* or *ARF8* transcript levels similar to or higher than those of *mARF6-II* or *mARF6-III* plants (Fig. 4A). A small proportion (less than 5%) of P_{35S}*::ARF6*, *gARF6* and *gARF8* plants also had small leaves. Thus, whereas an elevated *ARF6* expression level inhibited leaf growth, only a loss of *miR167* regulation caused flowers to be sterile.

miR167 regulates ovule development

Female sterility in *mARF6* plants arose from defects in ovule development. Early stage 2-IV ovules from *mARF6-II* plants had indistinguishable morphology from wild-type ovules, with inner and outer integuments initiated properly on ovule flanks (Fig. 4C,G). However, whereas wild-type outer integuments grew to encase the entire nucellus (Fig. 4D,E), *mARF6-II* outer integuments only grew slightly (Fig. 4H,I). In *mARF6-I* ovules, both inner and outer integuments and the nucellus were developmentally arrested (Fig. 4K). In *mARF6-III* ovules, outer integuments extended farther than in *mARF6-II* ovules, but they nevertheless failed to envelop the nucellus completely (Fig. 4L). In contrast to these effects on integument growth, cell morphology and arrangement in funiculi of *mARF6* ovules appeared normal (Fig. 4E,I).

These ovule integument defects affected both pollen tube guidance to the ovule and embryo development. Wild-type pollen tubes grew normally in transmitting tracts of *mARF6-II* gynoecia (Fig. 4M). However, only a small proportion of *mARF6* ovules (12%, n=195) were fertilized by wild-type pollen (Fig. 4F,J), whereas 84% (n=70) of *gARF6* ovules were fertilized. Moreover, fertilized *mARF6* ovules still failed to support embryo development. Seven days after pollination, *gARF6* embryos had developed to mid-torpedo stage (Fig. 4N), whereas embryos on *mARF6* plants were developmentally arrested at the four-cell stage (Fig. 4O). Embryos formed in self-fertilized *mARF6-III* flowers also developed only to the four-cell stage. Similarly, absence of the outer integument in the *inner no outer-1* (*ino-1*) mutant, which is deficient in a member of the *YABBY* gene family (Villanueva et al., 1999), caused reduced fertilization efficiency and arrested embryo development (data not shown). Thus, a primary defect in integument growth accounts for female sterility.

To determine whether altered distribution of *ARF6* and *ARF8* transcripts could account for these phenotypes, we examined *ARF6* and *ARF8* expression patterns in flowers of *mARF6-II* and *mARF8-II* plants by in situ hybridization (Fig. 1). As a second method, we also compared X-gluc staining patterns in plants carrying *miR167*-insensitive translational GUS fusions (*mARF6:GUS*, *mARF8:GUS*) with the staining patterns of the *gARF6:GUS* and *gARF8:GUS* plants described above (Fig. 2). In some strongly staining *mARF8:GUS* lines, a subset of ovules had reduced outer integument growth similar to *mARF6-III* ovules (Fig. 2N), suggesting that these constructs were partially functional. However, most *mARF6:GUS* and *mARF8:GUS* plants had fertile flowers, and these reporter constructs thereby revealed expression patterns largely independently of effects of the *mARF6* or *mARF8* mutations on ovule or anther development.

Consistent with northern blot results, *ARF6* expression in *mARF6-II* ovules appeared stronger in tissues where *ARF6* was expressed in wild-type ovules (Fig. 1E-F,H-I, Fig. 2C-E,H-J). Moreover, *mARF6* (Fig. 1H,I) and *mARF6:GUS* (Fig. 2H-J) expression also appeared in the integuments and nucellus. In stage 4-I ovules, staining of *mARF6:GUS* persisted most strongly in the chalazal domain of the mature ovule, but decreased in the tips of the integuments (Fig. 2J). In *mARF8* ovules, the expression of *ARF8* expanded only into the integuments and not into the nucellus (Fig. 1K), suggesting that the expanded expression of *ARF8* into the integument region might be sufficient to arrest outer integument growth. Similarly, *mARF8:GUS* was expressed in both funiculi and ovules (Fig. 2L,N).

INO was expressed in outer integuments of ovules, and *ino* mutations also caused arrested outer integument growth (Villanueva et al., 1999). However, *mARF6* ovules had a normal *INO* expression pattern, and *ino-1* ovules had a normal *ARF6* expression pattern (see Fig. S3 in the supplementary material), suggesting that *mARF6* affects integument growth independently of the INO pathway.

MIR167a is expressed in ovules and anthers

The *mARF6* and *mARF8* expression data indicated that *miR167* limits *ARF6* and *ARF8* transcript expression domains in ovules. To determine *MIR167* expression domains, we made transgenic plants carrying approximately 2 kb promoter fragments upstream of the stem-loop sequences of *MIR167a*, *b*, *c* and *d* fused to a *GFP-GUS* reporter gene ($P_{MIR167a,b,c,d}$*::GUS*), and analyzed promoter activities by X-gluc staining. In ovules, $P_{MIR167a}$*::GUS* expression (Fig. 2P-R), and to a lesser degree $P_{MIR167b}$*::GUS* and $P_{MIR167c}$*::GUS* expression (Fig. 2V,X), correlated with *miR167* functions revealed by mutating target sites. $P_{MIR167a}$*::GUS* expression first appeared at late ovule stage 1, in the cells from which both the inner and outer integuments would later be initiated (Fig. 2P). As both integuments enveloped the nucellus and the ovule began to grow asymmetrically, staining expanded into the entire nucellus and integuments, but was always absent from the funiculus (Fig. 2Q,R). $P_{MIR167a}$*::GUS* also stained in anthers and in sepal vasculature (Fig. 2O). $P_{MIR167b}$*::GUS* was expressed in the ovules and nectaries, but was not detected in other floral organs in the open flower (Fig. 2U), and staining in mature $P_{MIR167b}$*::GUS* ovules was restricted mostly to the tips of inner and outer integuments (Fig. 2V). $P_{MIR167c}$*::GUS* stained mainly in the stamen filaments with a trace amount of staining in the ovules (Fig. 2W,X), and $P_{MIR167d}$*::GUS* stained only in sepals and petals, but not in the internal floral organs (Fig. 2Y). In situ hybridization results have also shown that, in both *Nicotiana benthamiana* and *Arabidopsis*, *miR167* is present in ovules and in anther vasculature, but not in funiculi (Valoczi et al., 2006).

miR167 regulates anther development

Male sterility of *mARF6* and *mARF8* flowers was due to indehiscent anthers (Fig. 4B). Anthers of *mARF6* and *mARF8* flowers appeared normal before stage 10. However, *mARF6-II* anthers grew to be 20% larger than wild-type anthers as a result of enlarged connective cells, without any significant increase in cell number (Fig. 5A,D). By contrast, the vascular bundles of *mARF6-II* anthers were smaller than those of wild-type anthers (Fig. 5B,E). In the oldest closed wild-type flower bud, anther tapetum and septum had entirely degraded, and as flowers opened stomium cells broke apart to allow the release of pollen grains (Fig. 5A). In *mARF6-II* anthers, traces of tapetum were present within the anther locules of the oldest closed flower bud, and the septum did not degrade so that the two anther locules did not fuse. Septum cell breakage occurred in

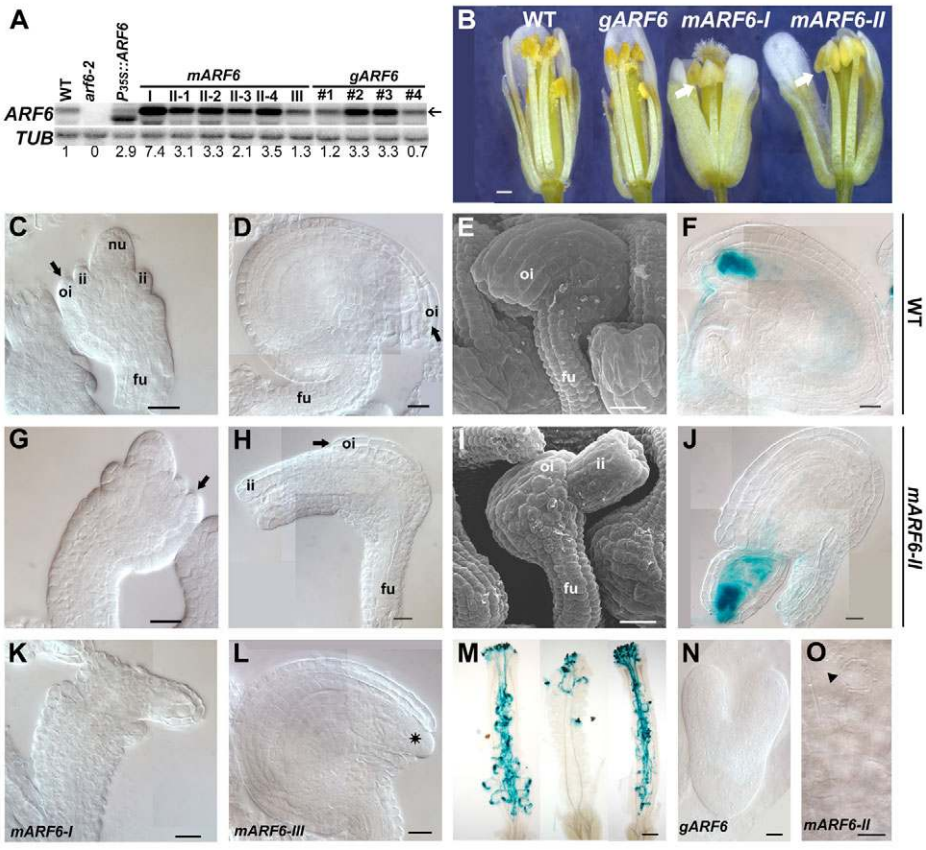

Fig. 4. *ARF6* expression, and flower and ovule phenotypes of *mARF6* plants. (**A**) Northern blot analysis of *ARF6* transcript levels in wild-type, *arf6-2*, P_{35S}*::ARF6*, and individual *mARF6* and *gARF6* transgenic plant flowers. The transcript of P_{35S}*::ARF6* is shorter because it lacks the 5′ and 3′ UTRs. Arrow indicates the *ARF6* transcript. Numbers beneath lanes indicate relative *ARF6* transcript levels normalized to the β-tubulin loading control. (**B**) Wild-type, *gARF6*, *mARF6-I* and *mARF6-II* flowers. Arrows indicate indehiscent anthers. (**C-E**,**G-I**) Wild-type (C-F) and *mARF6-II* (G-J) stage 2-IV (C,G) and stage 4-I (D,E,H,I) ovules. Arrows in C,D,G and H indicate outer integuments. (**K**) Stage 4-I *mARF6-I* ovule. (**L**) Stage 4-I *mARF6-III* ovule; asterisk indicates exposed embryo sac. (**F**,**J**,**M**) Wild-type (F,M left), *arf6 arf8* (M middle) and *mARF6-II* (J,M right) gynoecia (M) and ovules (F,J) after pollination with the pollen-specific reporter *LAT52:GUS* pollen (Johnson et al., 2004). (**N**,**O**) Embryos of *gARF6* (N) and *mARF6-II* (O) plants 7 days after pollination with wild-type pollen. Arrowhead in O indicates arrested embryo. fu, funiculus; ii, inner integument; oi, outer integument; nu, nucellus. Scale bars: 0.3 mm in B,M; 12 μm in C,D,F,G,H,J-L,N,O; 20 μm in E,I.

DEVELOPMENT

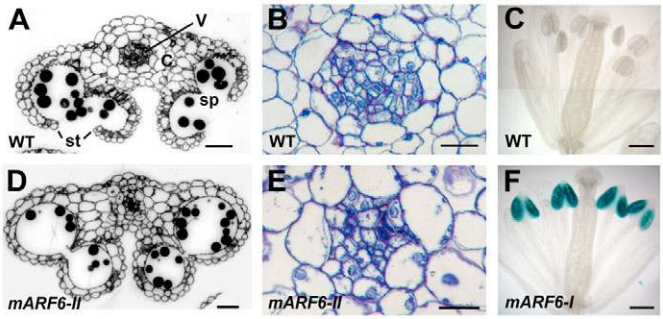

Fig. 5. Anther phenotypes of *mARF6* plants. (**A**) Anther from a stage 13 wild-type flower. c, connective cells; v, vascular bundle; sp, septum; st, stomium. (**D**) Anther from a stage 13 *mARF6-II* flower. (**B**,**E**) Enlarged views of anther vascular bundles and surrounding connective cells from A and D, respectively. (**C**,**F**) *DR5::GUS* staining patterns in wild-type (C) and *mARF6-I* (F) stage 13 flowers. Scale bars: 30 μm in A,D; 12 μm in B,E; 0.3 mm in C,F.

mARF6-II anthers after flower opening, but the stomium still remained intact, resulting in a lack of anther dehiscence (Fig. 5D). Unlike the *arf6 arf8* double mutant, spraying with JA did not restore *mARF6* anther dehiscence.

Whereas wild-type *ARF6* and *ARF8* were expressed in stamen filaments but not in anthers (Fig. 1C; Fig. 2A,B,K), *mARF6* and *mARF8* transcripts were also present in anther vasculature after floral stage 9 (Fig. 1G, data not shown). $P_{MIR167a}$*::GUS* was expressed in anther primordia as they differentiated, and throughout young anthers (Fig. 2S). As anthers matured, $P_{MIR167a}$*::GUS* expression became restricted to anther connective cells (Fig. 2T). We also transformed the *mARF6* construct into plants with the synthetic auxin-responsive reporter construct *DR5::GUS* (Ulmasov et al., 1997). In T1 plants showing *mARF6-I* phenotypes, we detected ectopic *DR5::GUS* expression in stage 13 flower anther locules, but not in vascular or connective cells (Fig. 5C,F).

DISCUSSION

miR167 regulates both female and male floral organ development. Loss of *miR167* regulation in *mARF6* and *mARF8* flowers expanded the domains of *ARF6* and *ARF8* expression, and caused arrested ovule development and anther indehiscence. Plants that overexpressed *ARF6* or *ARF8* but had normal *miR167* regulation were fertile, indicating that loss of *miR167*-regulated patterning of *ARF6* and *ARF8* gene expression, rather than a higher expression level, caused these phenotypes. *miR167* directs *ARF6* and *ARF8* transcript cleavage, but might also affect *ARF6* and *ARF8* transcription, as it has been shown that *miR165/166* decreases *PHB* and *PHV* transcription by promoting DNA methylation in the coding regions downstream of the miRNA target sites (Bao et al., 2004).

Of the four predicted *MIR167* genes, when overexpressed only *MIR167a* caused high *miR167* production and arrested flower development to the same extent as in *arf6 arf8* plants. DCL1 might recognize or process the stem-loop structure of *MIR167a* more efficiently than it does the others. In addition, *miR167b* and *miR167c* might have weaker activities toward *ARF6* and *ARF8* transcripts, and *MIR167d* may be a pseudogene that does not have activity. *MIR167a* is therefore most likely to be the main functional *miR167* precursor gene in vivo. Consistent with this idea, $P_{MIR167a}$*::GUS* expression in ovules correlated precisely with the *miR167* functions revealed in *mARF6* and *mARF8* plants.

In ovules, the complementary *ARF6*, *ARF8* and *miR167* expression patterns, and the arrested development of *mARF6* and *mARF8* integuments, indicate that *miR167* functions to clear *ARF6* and *ARF8* transcripts from cells that will become integuments, thereby allowing integument growth. Persistence of the expression patterns at later ovule stages suggests that *miR167* both establishes and maintains the correct pattern. *ARF2*, encoding another ARF protein, is normally expressed in the integuments and nucellus, and inhibits integument growth (Schruff et al., 2006). The ectopic ARF6 and ARF8 activity caused by blocking *miR167* function may therefore activate pathways that ARF2 normally activates to restrict integument growth. Future studies may reveal the extent to which different ARF proteins have different activities, and why different *ARF* genes are expressed in mutually exclusive domains.

In anthers, *miR167* was present in vascular cells where *mARF6* and *mARF8* accumulated (Valoczi et al., 2006), indicating that *miR167* patterns gene expression in anthers as it does in ovules. However, although anther vasculature was altered in *mARF6* and *mARF8* plants, the strongest anther phenotypes were in connective cells, which grew abnormally large, and in locules, which failed to break open to release pollen and, in some cases, ectopically expressed the auxin-responsive marker *DR5::GUS*. *mARF6* and *mARF8* therefore have non-cell-autonomous effects in anthers. Anther dehiscence requires a series of desiccation events (Ishiguro et al., 2001), and excess *ARF6* and *ARF8* transcripts in the vasculature might increase water uptake, leading to excess connective cell expansion and preventing dehiscence.

Although *miR167* accumulated in anther vasculature (Valoczi et al., 2006), we detected $P_{MIR167a}$*::GUS* expression in connective cells but not in vasculature. This difference suggests that *miR167* processing or stability may differ in different cell types, or that *miR167* may move between cells.

Just as ectopic *mARF6* and *mARF8* appear to act cell autonomously in ovules but non-cell autonomously in anthers, wild-type *ARF6* and *ARF8* appear to act autonomously in gynoecium transmitting tracts but non-automonously on anthers, by affecting JA production from other tissues (Nagpal et al., 2005). Moreover, *mARF6* and *mARF8* restrict growth in ovules, but cause extra growth in anthers. These observations suggest that ARF6 and ARF8 may activate distinct target genes in ovules and anthers.

In *Drosophila*, microRNAs have been suggested to function to reinforce transcriptional repression patterns (Stark et al., 2005). By contrast, the function of *miR167* to restrict distribution of its target transcripts is an essential patterning function that is not conferred by transcriptional controls of *ARF6* and *ARF8* alone. *miR165/166* also affects development by excluding expression of its target transcripts from the abaxial domain of lateral organs (Juarez et al., 2004; Kidner and Martienssen, 2004; Mallory et al., 2004b). In fact, the *miR165/166*-insensitive *phb-1d/+* mutant also has arrested outer integuments (Sieber et al., 2004), suggesting that both *miR165/166* and *miR167* might regulate common pathways during ovule formation.

miR167 is present in angiosperms and gymnosperms, but not in mosses, lycopods or ferns (Axtell and Bartel, 2005). Angiosperms and gymnosperms are seed plants, and form integuments around the female gametophyte that later form the seed coat. Gymnosperm male gametophytes are also surrounded by sterile cells that are similar to angiosperm anther connective cells (Gifford and Foster, 1988). The appearance of *miR167* in seed plants but not in lower plants therefore suggests that regulation by *miR167* could have arisen as plants evolved the formation of sporophytic structures that protect gametophytes.

We thank Punita Nagpal, Paul Reeves and Christine Ellis for performing some cloning steps; and Sara Ploense for microscopy training. This work was supported by U.S. National Science Foundation grant IBN-0344257.

Supplementary material

Supplementary material for this article is available at http://dev.biologists.org/cgi/content/full/133/21/4211/DC1

References

Allen, E., Xie, Z., Gustafson, A. M. and Carrington, J. C. (2005). microRNA-directed phasing during trans-acting siRNA biogenesis in plants. *Cell* **121**, 207-221.

Axtell, M. J. and Bartel, D. P. (2005). Antiquity of microRNAs and their targets in land plants. *Plant Cell* **17**, 1658-1673.

Baker, C. C., Sieber, P., Wellmer, F. and Meyerowitz, E. M. (2005). The early extra petals1 mutant uncovers a role for microRNA miR164c in regulating petal number in Arabidopsis. *Curr. Biol.* **15**, 303-315.

Bao, N., Lye, K. W. and Barton, M. K. (2004). MicroRNA binding sites in Arabidopsis class III HD-ZIP mRNAs are required for methylation of the template chromosome. *Dev. Cell* **7**, 653-662.

Bartel, D. P. (2004). MicroRNAs: genomics, biogenesis, mechanism, and function. *Cell* **116**, 281-297.

Chen, X. (2004). A microRNA as a translational repressor of APETALA2 in Arabidopsis flower development. *Science* **303**, 2022-2025.

Ellis, C. M., Nagpal, P., Young, J. C., Hagen, G., Guilfoyle, T. J. and Reed, J. W. (2005). AUXIN RESPONSE FACTOR1 and AUXIN RESPONSE FACTOR2 regulate senescence and floral organ abscission in Arabidopsis thaliana. *Development* **132**, 4563-4574.

Emery, J. F., Floyd, S. K., Alvarez, J., Eshed, Y., Hawker, N. P., Izhaki, A., Baum, S. F. and Bowman, J. L. (2003). Radial patterning of Arabidopsis shoots by class III HD-ZIP and KANADI genes. *Curr. Biol.* **13**, 1768-1774.

Floyd, S. K. and Bowman, J. L. (2004). Gene regulation: ancient microRNA target sequences in plants. *Nature* **428**, 485-486.

Gifford, E. M. and Foster, A. S. (1988). *Morphology and Evolution of Vascular Plants*. New York: W. H. Freeman.

Goldberg, R. B., Beals, T. P. and Sanders, P. M. (1993). Anther development: basic principles and practical applications. *Plant Cell* **5**, 1217-1229.

Hagen, G. and Guilfoyle, T. (2002). Auxin-responsive gene expression: genes, promoters and regulatory factors. *Plant Mol. Biol.* **49**, 373-385.

Hardtke, C. S. and Berleth, T. (1998). The Arabidopsis gene MONOPTEROS encodes a transcription factor mediating embryo axis formation and vascular development. *EMBO J.* **17**, 1405-1411.

Hardtke, C. S., Ckurshumova, W., Vidaurre, D. P., Singh, S. A., Stamatiou, G., Tiwari, S. B., Hagen, G., Guilfoyle, T. J. and Berleth, T. (2004). Overlapping and non-redundant functions of the Arabidopsis auxin response factors MONOPTEROS and NONPHOTOTROPIC HYPOCOTYL 4. *Development* **131**, 1089-1100.

Holt, B. F., 3rd, Boyes, D. C., Ellerstrom, M., Siefers, N., Wiig, A., Kauffman, S., Grant, M. R. and Dangl, J. L. (2002). An evolutionarily conserved mediator of plant disease resistance gene function is required for normal Arabidopsis development. *Dev. Cell* **2**, 807-817.

Ishiguro, S., Kawai-Oda, A., Ueda, J., Nishida, I. and Okada, K. (2001). The *DEFECTIVE IN ANTHER DEHISCENCE1* gene encodes a novel phospholipase A1 catalyzing the initial step of jasmonic acid biosynthesis, which synchronizes pollen maturation, anther dehiscence, and flower opening in Arabidopsis. *Plant Cell* **13**, 2191-2209.

Johnson, M. A., von Besser, K., Zhou, Q., Smith, E., Aux, G., Patton, D., Levin, J. Z. and Preuss, D. (2004). Arabidopsis hapless mutations define essential gametophytic functions. *Genetics* **168**, 971-982.

Jones-Rhoades, M. W. and Bartel, D. P. (2004). Computational identification of plant microRNAs and their targets, including a stress-induced miRNA. *Mol. Cell* **14**, 787-799.

Jones-Rhoades, M. W., Bartel, D. P. and Bartel, B. (2006). MicroRNAs and their regulatory roles in plants. *Annu. Rev. Plant Biol.* **57**, 19-53.

Juarez, M. T., Kui, J. S., Thomas, J., Heller, B. A. and Timmermans, M. C. (2004). microRNA-mediated repression of rolled leaf1 specifies maize leaf polarity. *Nature* **428**, 84-88.

Karimi, M., Inze, D. and Depicker, A. (2002). GATEWAY vectors for Agrobacterium-mediated plant transformation. *Trends Plant Sci.* **7**, 193-195.

Kasschau, K. D., Xie, Z., Allen, E., Llave, C., Chapman, E. J., Krizan, K. A. and Carrington, J. C. (2003). P1/HC-Pro, a viral suppressor of RNA silencing, interferes with Arabidopsis development and miRNA unction. *Dev. Cell* **4**, 205-217.

Kidner, C. A. and Martienssen, R. A. (2004). Spatially restricted microRNA directs leaf polarity through ARGONAUTE1. *Nature* **428**, 81-84.

Kurihara, Y. and Watanabe, Y. (2004). Arabidopsis micro-RNA biogenesis through Dicer-like 1 protein functions. *Proc. Natl. Acad. Sci. USA* **101**, 12753-12758.

Laufs, P., Peaucelle, A., Morin, H. and Traas, J. (2004). MicroRNA regulation of the CUC genes is required for boundary size control in Arabidopsis meristems. *Development* **131**, 4311-4322.

Lee, Y., Kim, M., Han, J., Yeom, K. H., Lee, S., Baek, S. H. and Kim, V. N. (2004). MicroRNA genes are transcribed by RNA polymerase II. *EMBO J.* **23**, 4051-4060.

Liscum, E. and Reed, J. W. (2002). Genetics of Aux/IAA and ARF action in plant growth and development. *Plant Mol. Biol.* **49**, 387-400.

Long, J. A. and Barton, M. K. (1998). The development of apical embryonic pattern in Arabidopsis. *Development* **125**, 3027-3035.

Mallory, A. C., Dugas, D. V., Bartel, D. P. and Bartel, B. (2004a). MicroRNA regulation of NAC-domain targets is required for proper formation and separation of adjacent embryonic, vegetative, and floral organs. *Curr. Biol.* **14**, 1035-1046.

Mallory, A. C., Reinhart, B. J., Jones-Rhoades, M. W., Tang, G., Zamore, P. D., Barton, M. K. and Bartel, D. P. (2004b). MicroRNA control of PHABULOSA in leaf development: importance of pairing to the microRNA 5′ region. *EMBO J.* **23**, 3356-3364.

Mallory, A. C., Bartel, D. P. and Bartel, B. (2005). MicroRNA-directed regulation of Arabidopsis AUXIN RESPONSE FACTOR17 is essential for proper development and modulates expression of early auxin response genes. *Plant Cell* **17**, 1360-1375.

Nagpal, P., Ellis, C. M., Weber, H., Ploense, S. E., Barkawi, L. S., Guilfoyle, T. J., Hagen, G., Alonso, J. M., Cohen, J. D., Farmer, E. E. et al. (2005). Auxin response factors ARF6 and ARF8 promote jasmonic acid production and flower maturation. *Development* **132**, 4107-4118.

Reinhart, B. J., Weinstein, E. G., Rhoades, M. W., Bartel, B. and Bartel, D. P. (2002). MicroRNAs in plants. *Genes Dev.* **16**, 1616-1626.

Rhoades, M. W., Reinhart, B. J., Lim, L. P., Burge, C. B., Bartel, B. and Bartel, D. P. (2002). Prediction of plant microRNA targets. *Cell* **110**, 513-520.

Sanders, P. M., Bui, A. Q., Weterings, K., McIntire, K. N., Hsu, Y. C., Lee, P. Y., Truong, M. T., Beals, T. P. and Goldberg, R. B. (1999). Anther developmental defects in Arabidopsis thaliana male-sterile mutants. *Sex Plant Reprod.* **11**, 297-322.

Schneitz, K., Hulskamp, M., Kopczak, S. D. and Pruitt, R. E. (1997). Dissection of sexual organ ontogenesis: a genetic analysis of ovule development in Arabidopsis thaliana. *Development* **124**, 1367-1376.

Schruff, M. C., Spielman, M., Tiwari, S., Adams, S., Fenby, N. and Scott, R. J. (2006). The AUXIN RESPONSE FACTOR 2 gene of Arabidopsis links auxin signalling, cell division, and the size of seeds and other organs. *Development* **133**, 251-261.

Schwab, R., Palatnik, J. F., Riester, M., Schommer, C., Schmid, M. and Weigel, D. (2005). Specific effects of MicroRNAs on the plant transcriptome. *Dev. Cell* **8**, 517-527.

Sessions, A., Nemhauser, J. L., McColl, A., Roe, J. L., Feldmann, K. A. and Zambryski, P. C. (1997). ETTIN patterns the Arabidopsis floral meristem and reproductive organs. *Development* **124**, 4481-4491.

Sessions, A., Weigel, D. and Yanofsky, M. F. (1999). The Arabidopsis thaliana MERISTEM LAYER 1 promoter specifies epidermal expression in meristems and young primordia. *Plant J.* **20**, 259-263.

Sieber, P., Gheyselinck, J., Gross-Hardt, R., Laux, T., Grossniklaus, U. and Schneitz, K. (2004). Pattern formation during early ovule development in Arabidopsis thaliana. *Dev. Biol.* **273**, 321-334.

Skinner, D. J., Hill, T. A. and Gasser, C. S. (2004). Regulation of ovule development. *Plant Cell* **16**, S32-S45.

Smyth, D. R., Bowman, J. L. and Meyerowitz, E. M. (1990). Early flower development in Arabidopsis. *Plant Cell* **2**, 755-767.

Stark, A., Brennecke, J., Bushati, N., Russell, R. B. and Cohen, S. M. (2005). Animal MicroRNAs confer robustness to gene expression and have a significant impact on 3′UTR evolution. *Cell* **123**, 1133-1146.

Sunkar, R., Girke, T., Jain, P. K. and Zhu, J. K. (2005). Cloning and characterization of microRNAs from rice. *Plant Cell* **17**, 1397.

Tian, Q., Nagpal, P. and Reed, J. W. (2003). Regulation of Arabidopsis SHY2/IAA3 protein turnover. *Plant J.* **36**, 643-651.

Tiwari, S. B., Hagen, G. and Guilfoyle, T. (2003). The roles of auxin response factor domains in auxin-responsive transcription. *Plant Cell* **15**, 533-543.

Ulmasov, T., Hagen, G. and Guilfoyle, T. J. (1997). ARF1, a transcription factor that binds to auxin response elements. *Science* **276**, 1865-1868.

Valoczi, A., Varallyay, E., Kauppinen, S., Burgyan, J. and Havelda, Z. (2006). Spatio-temporal accumulation of microRNAs is highly coordinated in developing plant tissues. *Plant J.* **47**, 140-151.

Villanueva, J. M., Broadhvest, J., Hauser, B. A., Meister, R. J., Schneitz, K. and Gasser, C. S. (1999). INNER NO OUTER regulates abaxial- adaxial patterning in Arabidopsis ovules. *Genes Dev.* **13**, 3160-3169.

Wang, J. W., Wang, L. J., Mao, Y. B., Cai, W. J., Xue, H. W. and Chen, X. Y. (2005). Control of root cap formation by MicroRNA-targeted auxin response factors in Arabidopsis. *Plant Cell* **17**, 2204-2216.

Williams, L., Grigg, S. P., Xie, M., Christensen, S. and Fletcher, J. C. (2005). Regulation of Arabidopsis shoot apical meristem and lateral organ formation by microRNA miR166g and its AtHD-ZIP target genes. *Development* **132**, 3657-3668.

Xie, Z., Allen, E., Fahlgren, N., Calamar, A., Givan, S. A. and Carrington, J. C. (2005). Expression of Arabidopsis MIRNA genes. *Plant Physiol.* **138**, 2145-2154.

Zuker, M. (2003). Mfold web server for nucleic acid folding and hybridization prediction. *Nucleic Acids Res.* **31**, 3406-3415.